Electronic Structure of Octahedral Copper(I) Cluster Complexes: $[H_6Cu_6(PH_3)_6]$ and $[CCu_6(PH_3)_6]^{2+}$

G. A. Bowmaker,[†,‡] M. Pabst,[§] N. Rösch,[*,§] and H. Schmidbaur[†]

Anorganisch-Chemisches Institut der Technischen Universität München, Lichtenbergstrasse 4, W-8046 Garching, Germany, Department of Chemistry, University of Auckland, Private Bag 92019, Auckland, New Zealand, and Lehrstuhl für Theoretische Chemie der Technischen Universität München, Lichtenbergstrasse 4, W-8046 Garching, Germany

Received July 31, 1992

The structure and bonding in the octahedral cluster complexes $[H_6Cu_6(PH_3)_6]$ and $[CCu_6(PH_3)_6]^{2+}$, and also in a number of related mononuclear and cluster phosphine complexes of copper, have been studied by the linear combination of Gaussian-type orbital local density functional (LCGTO–LDF) method. The metal–metal and metal–ligand bond lengths in $[H_6Cu_6(PH_3)_6]$ (Cu–Cu = 2.50; Cu–P = 2.12; Cu–H = 1.76 Å) agree closely with those of a recently reported X-ray crystallographic structure determination for the corresponding PPh_3 complex $[H_6Cu_6(PPh_3)_6]$. A value of 990 cm^{-1} is calculated for the as yet unmeasured totally symmetrical Cu–H stretching frequency in this complex. The corresponding frequency for $[H_6Cu_6]$, 1360 cm^{-1}, lies close to the value 1400 cm^{-1}, which has been tentatively assigned to the symmetrical vibrational mode of H atoms chemisorbed on triply bridging sites on copper metal. $[CCu_6(PH_3)_6]^{2+}$ has a minimum energy configuration (Cu–Cu = 2.63; Cu–P = 2.10; Cu–C = 1.86 Å) which is more stable than that of $[CCu_4(PH_3)_4] + 2[Cu(PH_3)]^+$ by 835 kJ mol^{-1}. A comparison with the calculated binding energy of $[CAu_6(PH_3)_6]^{2+}$ shows that the copper analogue should be almost as stable as the known cluster ion $[CAu_6(PPh_3)_6]^{2+}$. Electronic structure calculations were also carried out on the copper(I) complexes $[Cu(PH_3)_n]^+$ and on the copper(0) complexes $[Cu(PH_3)_n]^0$, n = 1–4, in the course of this study. Comparison of the results of the copper(I) complexes with those recently reported for the analogous NH_3 complexes reveals a greater stability for the three- and four-coordinate species with the phosphine ligand. The results for the copper(0) complexes show some unusual features which can be associated with a change in the nature of the HOMO from n = 1 to 2, and this behavior parallels that observed experimentally for the analogous ethylene complexes by matrix isolation EPR spectroscopy.

1. Introduction

The preparation and structure of the gold(I) complex cation $[CAu_6(PPh_3)_6]^{2+}$ has recently been reported.[1,2] This ion consists of an octahedron of six gold atoms surrounding a central carbon atom, with triphenylphosphine bound terminally to each gold atom. It has been proposed that gold–gold bonding, enhanced by the relativistic contraction of the gold 6s orbital, plays an important role in stabilizing this cluster compound.[1,3] Molecular orbital (MO) calculations carried out on $[CAu_6(PH_3)_6]^{2+}$ and related model systems suggest that the strength of the gold–gold interaction is related to the decrease in the gold 5d valence shell population from the value 10 expected for a closed (nonbonding) $5d^{10}$ shell.[3–6]

A structure related to that of the gold cluster complex described above is shown by the copper(I) hydride complex $[H_6Cu_6(PPh_3)_6]$ and analogues containing differently substituted phosphine ligands.[7–13] These compounds contain an octahedron of six copper atoms with one phosphine ligand terminally bound to each copper atom. The earlier structural studies failed to locate the hydride hydrogen atoms, and previous attempts to predict the location of these atoms by a localized bond treatment yielded ambiguous results, mainly because the nature of the bonding in such complexes was poorly understood.[9] In particular, the importance of copper–copper bonding is uncertain.[8] For three such complexes, structural studies have now shown that the hydride H atoms are situated in six face-bridging positions of the Cu_6 octahedron, rather than in edge-bridging positions, which was considered to be another likely possibility.[11–13]

The close structural relationship between the above gold(I) and copper(I) cluster complexes has prompted us to study whether there is a similar close relationship between the electronic structure and bonding in these species. Consider first the octahedral $[M_6(PPh_3)_6]$ unit. This is a species which would exhibit M–M bonds built from metal sp orbitals that contain the 6 valence s electrons of the M atoms. Since the metal atoms have a formal oxidation state of zero in this unit, the cluster is very electron-rich, and an increase in stability is expected if some of the occupied higher energy orbitals were stabilized by bonding to a suitable additional atom (or several of them). In the gold(I) cluster $[CAu_6(PPh_3)_6]^{2+}$ this is achieved by the central C^{2+} unit which formally can take up 6 electrons. In the copper(I) cluster $[H_6Cu_6(PPh_3)_6]$ the 6 H atoms can act in an analogous way. Of course, the addition of these atoms results in a change in the bonding character of the

* Author to whom correspondence should be addressed.
† Anorganisch-Chemisches Institut der Technischen Universität München.
‡ Permanent address: University of Auckland.
§ Lehrstuhl für Theoretische Chemie der Technischen Universität München.

(1) Scherbaum, F.; Grohmann, A.; Huber, B.; Krüger, C.; Schmidbaur, H. *Angew. Chem.* **1988**, *100*, 1602; *Angew. Chem., Int. Ed. Engl.* **1988**, *27*, 1544.
(2) Schmidbaur, H.; Brachthäuser, B.; Steigelmann, O. *Angew. Chem.* **1991**, *103*, 1552; *Angew. Chem., Int. Ed. Engl.* **1991**, *30*, 1488.
(3) Rösch, N.; Görling, A.; Ellis, D. E.; Schmidbaur, H. O. *Angew. Chem.* **1989**, *101*, 1410; *Angew. Chem., Int. Ed. Engl.* **1989**, *28*, 1357.
(4) Görling, A.; Rösch, N.; Ellis, D. E.; Schmidbaur, H. *Inorg. Chem.* **1991**, *30*, 3986.
(5) Mingos, D. M. P. *J. Chem. Soc., Dalton Trans.* **1976**, 1163.
(6) Pyykkö, P.; Zhao, Y.-F. *Chem. Phys. Lett.* **1991**, *177*, 103.
(7) Bezman, S. A.; Churchill, M. R.; Osborn, J. A.; Wormald, J. *J. Am. Chem. Soc.* **1971**, *93*, 2063.
(8) Churchill, M. R.; Bezman, S. A.; Osborn, J. A.; Wormald, J. *Inorg. Chem.* **1972**, *11*, 1818.
(9) Ho, D. M.; Bau, R. *Inorg. Chim. Acta* **1984**, *84*, 213.
(10) Zerger, R.; Rhine, W.; Stucky, W. *J. Am. Chem. Soc.* **1974**, *96*, 6048.
(11) Lemmen, T. H.; Folting, K.; Huffman, J. C.; Caulton, K. G. *J. Am. Chem. Soc.* **1985**, *107*, 7774.
(12) Stevens, R. C.; McLean, M. R.; Bau, R.; Koetzle, T. F. *J. Am. Chem. Soc.* **1989**, *111*, 3472.
(13) Albert, C. F.; Healy, P. C.; Kildea, J. D.; Raston, C. L.; Skelton, B. W.; White, A. H. *Inorg. Chem.* **1989**, *28*, 1300.

0020-1669/93/1332-0880$04.00/0

molecular orbitals occupied by these 6 electrons from Au–Au or Cu–Cu to Au–C or Cu–H. However, in the case of $[CAu_6(PPh_3)_6]^{2+}$, it has been shown that the situation is intermediate between these two extremes and that the cluster is stabilized by a combination of Au–Au and Au–C bonding.[3,4] The aim of the present work was to compare the electronic structures in the two types of complexes described above, with a particular emphasis on determining the relative importance of metal–ligand and metal–metal bonding. An additional aim was to examine the stability of related but as yet unknown complexes such as $[CCu_6(PPh_3)_6]^{2+}$.

To this end, electronic structure calculations were carried out on the model complexes (all of D_{3d} symmetry) $[Cu_6(PH_3)_6]$, $[H_6Cu_6]$, $[H_6Cu_6(PH_3)_6]$, and $[CCu_6(PH_3)_6]^{2+}$, as well as on the species Cu_6, $[CCu_6]^{2+}$ (O_h symmetry), and $[CCu_4(PH_3)_4]$ (T_d symmetry). The results were also compared to those obtained for the corresponding gold complexes $[Au_6(PH_3)_6]$, $[CAu_6(PH_3)_6]^{2+}$, and $[CAu_6]^{2+}$.

The complexes were studied with the linear combination of Gaussian-type orbitals local density functional (LCGTO–LDF) method.[14] In the case of $[H_6Cu_6(PH_3)_6]$, which is a model for the known compound $[H_6Cu_6(PPh_3)_6]$, the quality of the calculations can be checked by comparing the calculated and observed molecular geometries. Also, the Cu–H vibrational frequencies of the latter compound have never been determined, and it is of interest to see whether these could be predicted. The LCGTO–LDF method has been used successfully to calculate vibrational frequencies of atoms and small molecules bonded to metal clusters and metal surfaces.[14b,15,16] A scalar-relativistic version of LCGTO–LDF is available[17a,b] which has recently been implemented for molecular systems.[17c,d] This method has been applied to the relevant gold complexes[17c] in order to supplement the previous Xα(DV Xα) investigations[3,4,18] on these compounds by a geometry optimization and by binding energies. This work will be presented in detail elsewhere[17c] and will be used here only for comparison.

Also, calculations were carried out on simple mononuclear copper phosphine complexes $[Cu(PH_3)_n]^+$ and $[Cu(PH_3)_n]^0$ (n = 1–4) in order to obtain more information about Cu–P bonding and the effect which this has on the stability of the Cu_6 clusters.

2. Computational Details

In the LCGTO–LDF method one solves the effective one-electron equations of the Kohn–Sham approach to density functional theory self-consistently at the level of the local density approximation.[19] Bond lengths and vibrational frequencies may be obtained with good accuracy in the LDF approximation, but binding energies often turn out too large compared to experiment.[19] Corrections to the binding energy can be calculated with the help of improved energy functionals, which incorporate gradients of the electronic density,[19c] but they have not been included in this study.

Symmetrized linear combinations of Gaussian-type orbitals are employed to describe the molecular orbitals.[14] In addition, auxiliary Gaussian functions are used to represent the molecular density and the exchange-correlation potential. In the present investigation, the latter was employed in the parametrization suggested by Vosko, Wilk, and Nusair.[20] For open-shell systems, the method was applied in its spin-polarized version. For Cu, a (15s,11p,6d) MO basis was used which was

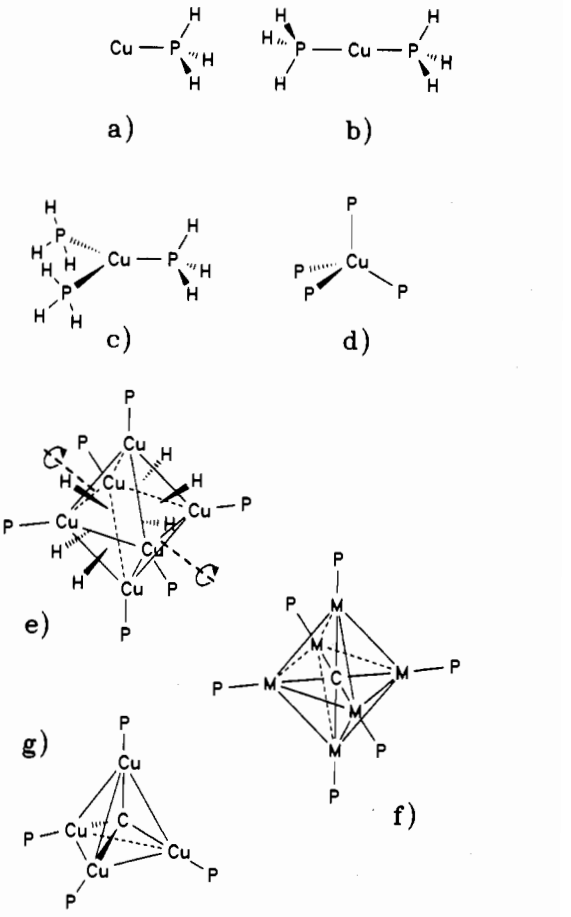

Figure 1. Structures of some of the systems studied: (a) $[Cu(PH_3)]^{q+}$ (C_{3v}); (b) $[Cu(PH_3)_2]^{q+}$ (D_{3d}); (c) $[Cu(PH_3)_3]^{q+}$ (C_{3v}); (d) $[Cu(PH_3)_4]^{q+}$ (T_d); (e) $[H_6Cu_6(PH_3)_6]$ (D_{3d}); (f) $[CM_6(PH_3)_6]^{2+}$, M = Cu, Au (D_{3d}); (g) $[CCu_4(PH_3)_4]$ (T_d). The point group symmetry for each species is given in parentheses. The phosphine hydrogen atoms are displayed only for the first three compounds.

derived from an atomic basis[21a] by adding one s-exponent (0.3305), two diffuse p-exponents (0.265, 0.0991) and one d-exponent (0.1491).[21b] This basis set was contracted to [6s,4p,3d]. For P, a MO basis set of the type (12s,9p,1d)[21c] contracted to [6s,4p,1d], was used; for C a (9s,5p,1d) MO basis[21d] was only slightly contracted to [7s,4p,1d] to allow more flexibility for the central atom of the octahedral cluster. For H, a (6s,1p) basis[21d] was contracted to [4s,1p]. Polarization functions were added in the MO basis sets of P, C, and H.[21e] The auxiliary basis sets for fitting the charge density and the exchange-correlation functions were constructed by properly scaling the MO exponents and by adding p-type polarization functions.[22]

The structures of the systems studied are illustrated in Figure 1. All metal M_6 units were kept in a local octahedral structure in order to significantly reduce the computational effort. In the case of $[H_6Cu_6(PH_3)_6]$ this is certainly an approximation since two rather different Cu–Cu distances are found experimentally in $[H_6Cu_6(PPh_3)_6]$,[13] one within each of the two triangular Cu_3 units (2.48 Å) and one between the two "trans" faces, which are not capped by a hydrogen atom (2.73 Å). The equilibrium geometries for the various copper compounds and the force constants were determined by fitting Tchebychev polynomials to the energies evaluated at five different geometries for each investigated degree of freedom. In cases of more than one degree of freedom, the optimization was carried out consecutively. Optimized geometries were

(14) (a) Dunlap, B. I.; Rösch, N. *J. Chim. Phys. Physico-chim. Biol.* **1989**, *86*, 671. (b) *Adv. Quantum Chem.* **1990**, *21*, 317.
(15) Rösch, N.; Ackermann, L.; Pacchioni, G. *J. Am. Chem. Soc.* **1992**, *29*, 2901.
(16) Mijoule, C.; Bouteiller, Y.; Salahub, D. R. *Surf. Sci.* **1990**, *253*, 375.
(17) (a) Knappe, P.; Rösch, N. *J. Chem. Phys.* **1990**, *92*, 1153. (b) Häberlen, O.; Rösch, N. *J. Chem. Phys.* **1992**, *96*, 6322. (c) Rösch, N.; Häberlen, O. To be published. (d) Häberlen, O. D.; Rösch, N. *Chem. Phys. Lett.* **1992**, *199*, 491.
(18) Rosén, A.; Ellis, D. E. *J. Chem. Phys.* **1975**, *62*, 3039. Rosén, A.; Ellis, D. E.; Adachi, A.; Averill, F. W. *Chem. Phys.* **1976**, *65*, 3629.
(19) (a) Parr, R. G.; Yang, W. *Density Functional Theory of Atoms and Molecules*; Oxford University Press: New York, 1989. (b) Trickey, S. B., Ed. *Density Functional Theory of Many-Fermion Systems. Adv. Quantum Chem.* **1990**, *21*. (c) Ziegler, T. *Chem. Rev.* **1992**, *91*, 651.
(20) Vosko, S. H.; Wilk, L.; Nusair, M. *Can. J. Phys.* **1980**, *58*, 1200.
(21) (a) Wachters, A. J. H. *J. Chem. Phys.* **1970**, *52*, 1033. (b) Hay, P. J. *J. Chem. Phys.* **1977**, *66*, 4377. (c) Veillard, A. *Theoret. Chim. Acta* **1968**, *12*, 405. (d) van Duijneveldt, F. B. *IBM Res. Rep.* **1991**, *RJ 945*. (e) Huzinaga, S. *Gaussian Basis Sets for Molecular Calculations*; Elsevier: Amsterdam, 1984.
(22) Jörg, H.; Rösch, N.; Sabin, J. R.; Dunlap, B. I. *Chem. Phys. Lett.* **1985**, *144*, 529. Rösch, N.; Knappe, P.; Sandl, P.; Görling, A.; Dunlap, B. I. In *The Challenge of d and f electrons. Theory and Computation.*; Salahub, D. R., Zerner, M. C., Eds.; ACS Symposium Series NO. 294; American Chemical Society: Washington, DC, 1989; p 180.

Table I. Cu–P Bond Lengths (r_e in Å), Force Constants (k_e in N m^{-1}) and Totally Symmetric Vibrational Frequencies (ν_e in cm^{-1}) in $[Cu(PH_3)_n]^{q+}$ (n = 1–4; q = 1, 0)

species	r_e	k_e	ν_e	species	r_e	k_e	ν_e
$[Cu(PH_3)]^+$	2.14	177	362	$[Cu(PH_3)]$	2.19	132	292
$[Cu(PH_3)_2]^+$	2.17	159	282	$[Cu(PH_3)_2]$	2.11	193	315
$[Cu(PH_3)_3]^+$	2.17	209	319	$[Cu(PH_3)_3]$	2.13	272	364
$[Cu(PH_3)_4]^+$	2.21	124	245	$[Cu(PH_3)_4]$	2.23	95	223

used for the gold clusters which were obtained by scalar-relativistic calculations.[17c] The Au–Au (Au–P) distances were 2.940 (2.256), 2.748 (2.296) 2.895, and 2.705 Å in the clusters $[CAu_6(PPh_3)_6]^{2+}$, $[Au_6(PPh_3)_6]^{2+}$, $[CAu_6]^{2+}$, and $[Au_6]^{2+}$, respectively; the average of the experimentally observed values for $[CAu_6(PPh_3)_6]^{2+}$ is 3.005 Å for Au–Au and 2.272 Å for Au–P.[1] The PH_3 moieties were held in the experimentally observed geometry of the free molecule (P–H = 1.415 Å; H–P–H = 93.3°).[23] They were oriented such that the overall symmetry of the cluster was as high as possible. This allows the M_6 phosphine complexes to retain D_{3d} symmetry and maintain the equivalence of all of the metal and phosphorus atoms.

3. Results and Discussion

3.1. Mononuclear Systems. The Cu–P bond lengths and ν(Cu–P) vibrational frequencies obtained for the mononuclear copper phosphine complexes $[Cu(PH_3)_n]^+$ and $[Cu(PH_3)_n]^0$ (n = 1–4) are given in Table I. None of these species have been unambiguously identified experimentally, some evidence for the existence of $[Cu(PH_3)_n]^0$ species has been obtained from matrix isolation infrared spectroscopy. However, the structure of the $[Cu(PMe_3)_4]^+$ ion in a number of crystalline salts has recently been determined by X-ray diffraction.[25,26] These experimental Cu–P bond lengths of 2.27 Å (average) are close to the value 2.21 Å calculated here for $[Cu(PH_3)_4]^+$ confirming the general experience that d metal–ligand bonds are calculated too short and too strong in the LDF approximation. The progressive increase in the Cu–P bond length with increasing coordination number n in $[Cu(PH_3)_n]^+$ is as expected. The frequency of the totally symmetric Cu–P stretching mode of $[Cu(PH_3)_4]^+$ (ν(Cu–P) = 245 cm^{-1}) may be compared to the ν(Ni–P) frequencies in the isoelectronic Ni^0 complexes $[Ni(PH_3)_4]$ (300 cm^{-1})[27a] and $\{Ni[P(CH_3)_3]_4\}$ (196 cm^{-1});[27b] in order to provide a more direct link with these experimental observations, a calculation was also carried out for $[Ni(PH_3)_4]$ which gave Ni–P = 2.12 Å and ν(Ni–P) = 377 cm^{-1}.[28] It should be possible to stabilize the cation $[Cu(PH_3)_4]^+$ as a salt with a suitable anion and to measure its vibrational spectrum in order to provide a check on the results of the calculations reported here.

The results for the $[Cu(PH_3)_n]^0$ species exhibit some unusual features which may be rationalized in terms of the ground-state electron configuration (see the various MO energy level diagram in Figure 2). In $[Cu(PH_3)]$ the HOMO is the antibonding member of the pair of σ molecular orbitals formed by combination of the PH_3 lone pair donor orbital with the copper 4s orbital. The increase in the Cu–P bond length from $[Cu(PH_3)]^+$ to $[Cu(PH_3)]^0$ is therefore readily accounted for since the additional electron in the neutral species occupies a Cu–P antibonding MO. In $[Cu(PH_3)_2]$, however, there is a greater degree of overlap between the PH_3 lone pair donor orbital and the Cu 4s orbital such that the resulting σ_g antibonding orbital ($4a_{1g}$) ends up empty above the π_u HOMO ($2e_u$), which has Cu 4p rather than 4s character.

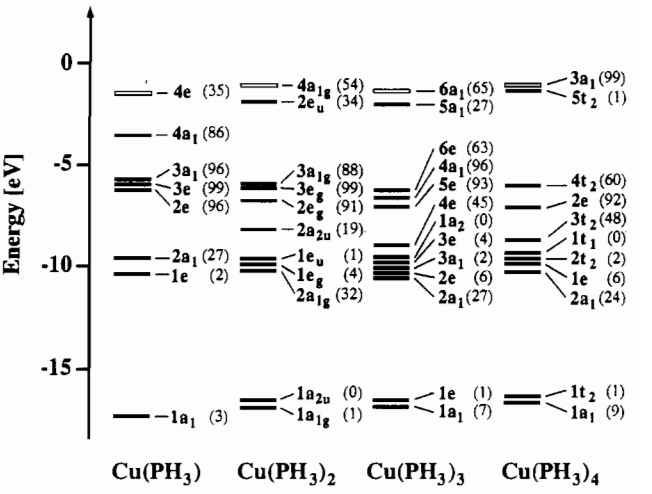

Figure 2. Valence energy levels of $[Cu(PH_3)_n]$. Occupied levels are displayed as a solid line; the LUMO is shown as a light line. The numbers in parentheses indicate the Mulliken population of Cu in percent.

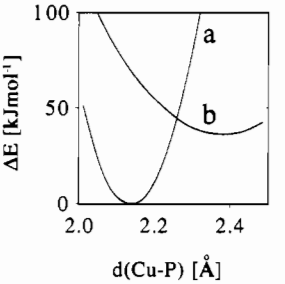

Figure 3. Potential energy curves for $[Cu(PH_3)_2]$: (a) ground state (unpaired electron in the HOMO, $2e_u$); (b) first excited state (unpaired electron in the $4a_{1g}$ MO).

The $2e_u$ orbital is nonbonding but acquires some bonding character via a π-interaction with ligand orbitals of P–H bonding character.

The HOMO changes its character from Cu–P antibonding in $[Cu(PH_3)]$ to bonding in $[Cu(PH_3)_2]$, and this accounts for the decrease in bond length from $[Cu(PH_3)]$ to $[Cu(PH_3)_2]$. In $[Cu(PH_3)_2]$, the state in which the σ_g antibonding orbital $4a_{1g}$ is occupied is not far above the ground state (see Figure 3); it even becomes the lowest energy state at longer Cu–P bond distances. For $[Cu(PH_3)_3]$, the HOMO ($5a_1$ in Figure 2) is similar in character to that of $[Cu(PH_3)_2]$, i.e. a bonding orbital involving the Cu $4p_z$ and the ligand orbitals of π-symmetry with respect to the Cu–P axes.

The change in the HOMO character from one involving mainly Cu 4s in $[Cu(PH_3)]$ to one of mainly Cu 4p in $[Cu(PH_3)_2]$ and $[Cu(PH_3)_3]$ should be detectable by EPR measurements on matrix-isolated species. Such an experiment has not yet been reported, but matrix-isolation EPR studies of the ethylene complexes $[Cu(C_2H_4)_n]$ show[29] that these species undergo a change in character of the ground state at n = 2 which is of the same type as that calculated here for the phosphine complexes. Also, studies of the Cu/CO system[30] have shown that the ground state for the complex $[Cu(CO)_3]$ is analogous to that calculated here for $[Cu(PH_3)_3]$.

In the tetrahedrally coordinated complex $[Cu(PH_3)_4]$ there is a further change in the ground-state configuration. The Cu 4s and 4p orbitals form bonding and antibonding molecular orbitals by interaction with ligand σ orbitals of the appropriate symmetry (a_1 and t_2, respectively). The bonding partners of them are filled whereas the antibonding combinations lie all above the lowest

(23) Weast, R. C., Ed. *Handbook of Chemistry and Physics*, 61st ed.; CRC Press: Boca Raton, FL, 1980.
(24) Bowmaker, G. A. *Aust. J. Chem.* **1978**, *31*, 2549.
(25) Dempsey, D. F.; Girolami, G. S. *Organometallics* **1988**, *7*, 1208.
(26) Bowmaker, G. A.; Healy, P. C.; Engelhardt, L. M.; Kildea, J. D.; Skelton, B. W.; White, A. H. *Aust. J. Chem.* **1990**, *43*, 1697.
(27) (a) Trabelsi, M.; Loutellier, A.; Bigorgne, M. *J. Organomet. Chem.* **1972**, *40*, C45. Trabelsi, M.; Loutellier, A. *J. Mol. Struct.* **1978**, *43*, 151. (b) Klein, H. F.; Schmidbaur, H. *Angew. Chem.* **1970**, *82*, 885.
(28) Pabst, M.; Rösch, N. Unpublished results.
(29) Howard, J. A.; Joly, H. A.; Mile, B. *J. Phys. Chem.* **1990**, *94*, 1275.
(30) Howard, J. A.; Mile, B.; Morton, J. R.; Preston, K. F.; Sutcliffe, R. *Chem. Phys. Lett.* **1985**, *117*, 115; *J. Phys. Chem.* **1986**, *90*, 1033. Howard, J. A.; Mile, B.; Morton, J. R.;

Table II. Mean Cu–P Bond Energies $\Delta E_1/n$ and Energies ΔE_2 of Addition of the nth Ligand for $[Cu(PH_3)_n]^{+q}$ (q = 1, 0) in kJ mol^{-1} [a]

	$[Cu(PH_3)_n]^+$		$[Cu(PH_3)_n]^0$	
n	$\Delta E_1/n$	ΔE_2	$\Delta E_1/n$	ΔE_2
1	−314	−314	−104	−104
2	−277	−241	−78	−52
3	−240	−166	−118	−197
4	−199	−76	−73	−61

[a] See text.

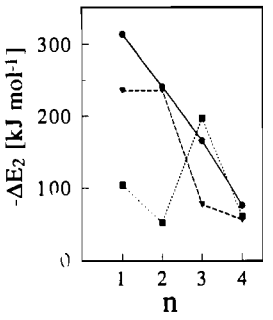

Figure 4. Energy of addition of the nth ligand in $[Cu(PH_3)_n]^+$ (●), $[Cu(PH_3)_n]^0$ (■), and $[Cu(NH_3)_n]^+$ (▼) (from ref 31).

lying vacant ligand orbitals. Thus, the remaining unpaired electron occupies an orbital which is entirely ligand-based ($5t_2$; see Figure 2). The first excited configuration with the unpaired electron residing in a Cu 4s-derived MO exhibits a shorter Cu–P bond length (2.19 Å). The corresponding energy minimum is calculated 36 kJ mol^{-1} above the ground state.

The calculated energy changes for the reactions

$$Cu^{q+} + nPH_3 \rightarrow [Cu(PH_3)_n]^{q+} \quad \Delta E_1 \qquad (1)$$

$$[Cu(PH_3)_{n-1}]^{q+} + PH_3 \rightarrow [Cu(PH_3)_n]^{q+} \quad \Delta E_2 \qquad (2)$$

(n = 1–4; q = 1, 0) are given in Table II. The quantity $\Delta E_1/n$ is the mean Cu–P bond energy in $[Cu(PH_3)_n]^{q+}$, while the differential bond energy ΔE_2 is the energy for the addition of the nth PH_3 in $[Cu(PH_3)_n]^{q+}$. In the case of $[Cu(PH_3)_n]^+$, ΔE_2 decreases smoothly with increasing n. This result is compared in Figure 4 with that obtained in a recently published calculation for the complexes $[Cu(NH_3)_n]^+$,[31] where ΔE_2 decreases in magnitude more markedly between n = 2 and n = 3, thus indicating a greater relative stability for the three- and four-coordinated species with the phosphine ligand. In the case of $[Cu(PH_3)_n]^0$, the variation of ΔE_2 with n is more complex, and this can be attributed to changes in the nature of the HOMO between n = 1 and 2 and between n = 3 and 4, as discussed above. Taking into account the method-based general overestimation of binding energies, the results suggest that the three-coordinated complex is the most stable; little further stabilization is achieved by addition of a fourth PH_3 ligand. This finding compares well with experimental observations on other $[CuL_n]^0$ complexes (L = CO, C_2H_4) where the tricoordinated species are the most stable.[29,30] Complexes with n = 4 have not been observed. Of the $[Cu(PH_3)_n]^{q+}$ species considered here, the cases for n = 1 are directly relevant for the calculations on the copper complexes (see below).

3.2. Copper Clusters. The equilibrium bond lengths calculated for the various copper cluster species are given in Table III. Also shown are the totally symmetric vibrational frequencies as derived from the force constants for the corresponding bonds. In the case of the Cu–H vibrations in the copper hydride clusters, this should be a very good approximation because the Cu–H modes are so high in frequency that they do not couple with any other cluster modes. In Table IV the energy changes for reactions resulting in the formation of the various copper clusters are collected.

In recent years, the electronic structure of copper clusters Cu_n (n = 2–5) has been the topic of a large number of theoretical investigations, based on ab initio as well as density functional methods.[32-36] In the present study, calculations were carried out on the bare clusters Cu_4 (T_d symmetry) and Cu_6 (O_h symmetry) as part of the evaluation of the Cu basis set contraction procedure and also to provide data for comparison with other species which contain these clusters. Since these are open-shell systems, it is unlikely that their equilibrium geometries correspond to the tetrahedral and octahedral structures to which they were constrained in this work. In the case of Cu_4, it has been shown by ab initio calculations that the equilibrium geometry is a planar trapezoidal one of D_{2h} symmetry.[33,36] The Cu–Cu distance calculated here for Cu_4 in T_d symmetry (2.32 Å) lies at the low end of the range (2.31–2.47 Å) of values found for D_{2h} symmetry.[33,36b] This tendency is in line with previously reported results for the dimer Cu_2. In a LCGTO–LDF calculation[35] a value of 2.21 Å was found, in very good agreement with experiment (2.22 Å)[36] but significantly shorter than ab initio calculations comparable to the ones cited above (2.28 Å).[33,36a] Not unexpectedly, one finds an increase of the Cu–Cu bond length in Cu_n with increasing n; the value in metallic copper is 2.54 Å. A very similar trend has been found in a recent LCGTO–LDF study on naked nickel clusters Ni_n (n = 6–44).[37]

The formation of the $[Cu_6(PH_3)_6]$ cluster from $[Cu(PH_3)]$ is quite exoenergetic, even more energy being released than in the formation of Cu_6 from Cu atoms. The formation of $[Cu_6(PH_3)_6]$ from Cu_6 and PH_3 is significantly less exoenergetic; the average energy released per PH_3 molecule is only slightly higher than that in the formation of the $[Cu(PH_3)]$ monomer (Tables II and IV). These results suggest that the cluster $[Cu_6(PH_3)_6]$ is held together by Cu–Cu bonds, which are of a strength comparable to those in Cu_6; an analogous conclusion has been reached for the corresponding gold clusters.[4] (The accuracy of the binding energies obtained by the LDF method precludes a more stringent statement.) Note that the results for the geometry and the force constants indicate a weakening of the Cu–Cu bonds when going from Cu_6 to $[Cu_6(PH_3)_6]$ (Table III).

In conjunction with the investigation of the copper hydride clusters, a calculation was carried out on the diatomic molecule CuH for which spectroscopic data are available.[38] The calculated CuH observables (Table III) are in very good agreement with experiment, much closer than those reported recently from a calculation using the modified coupled pair functional method (Cu–H = 1.51 Å; ν_e = 1852 cm^{-1})[39] or from one using the relativistic effective core potential method (Cu–H = 1.56 Å).[40] We calculate a binding energy D_e of −303 kJ mol^{-1}, in good agreement with experiment (−275 kJ mol^{-1})[38] but somewhat "overbound" as expected from the LDF approximation.

The energy released in the formation of the cluster $[H_6Cu_6]$ from CuH is about as large as the one in the formation of Cu_6 from Cu atoms (Table IV). In the case of $[H_6Cu_6]$, however, additional Cu–H bonds form as the bonding mode of the hydrogen

(31) Bauschlicher, C. W.; Langhoff, S. R.; Partridge, H. *J. Chem. Phys.* **1991**, *94*, 2068.

(32) Delley, B.; Ellis, D. E.; Freeman, A. J.; Bearends, E. J.; Post, D. *Phys. Rev.* **1983**, *B27*, 2132.

(33) Flad, J.; Igel-Mann, G.; Preuss, H.; Stoll, H. *Chem. Phys.* **1984**, *90*, 257.

(34) Wang, S.-W. *J. Chem. Phys.* **1985**, *82*, 4633.

(35) Salahub, D. R. *Adv. Chem. Phys.* **1987**, *69*, 447.

(36) (a) Bauschlicher, C. W.; Langhoff, S. R.; Partridge, H. *J. Chem. Phys.* **1989**, *91*, 2412. (b) *J. Chem. Phys.* **1990**, *93*, 8133.

(37) Rösch, N.; Ackermann, L.; Pacchioni, G. *Chem. Phys. Lett.* **1992**, *199*, 275.

(38) Huber, K. P.; Herzberg, G. *Constants of Diatomic Molecules*; D. Van Nostrand: New York, 1979.

(39) Chong, D. P.; Langhoff, S. R.; Bauschlicher, C. W.; Walch, S. P.; Partridge, H. *J. Chem. Phys.* **1986**, *85*, 2850.

(40) Flurer, R. A.; Busch, K. L. *J. Am. Chem. Soc.* **1991**, *113*, 3656.

Table III. Calculated Bond Lengths (r_e in Å) and Totally Symmetric Vibrational Frequencies (ν_e in cm^{-1}) for Copper Clusters and Related Species and Comparison with Experimental Data Where Available[a]

		r_e			ν_e		
sym	species	Cu–Cu	Cu–P	Cu–H	Cu–Cu	Cu–P	Cu–H
T_d	Cu_4	2.32			301		
O_h	Cu_6	2.35			293		
D_{3d}	$[Cu_6(PH_3)_6]$	2.40	2.10		238	354	
$C_{\infty v}$	CuH			1.44			1984
	expt[b]			1.46			1941
D_{3d}	$[H_6Cu_6]$	2.41		1.75	282		1363
D_{3d}	$[H_6Cu_6(PH_3)_6]$	2.50	2.12	1.76	206	296	989
	expt[c]	2.48 (2.74)	2.23	1.75			
O_h	$[CCu_6]^{2+}$	2.62			245		
D_{3d}	$[CCu_6(PH_3)_6]^{2+}$	2.63	2.10		248	366	
T_d	$[CCu_4]$	2.90			274		
T_d	$[CCu_4(PH_3)_4]$	3.01	2.14		291	428	

[a] The vibrational frequencies have been calculated from the corresponding force constants neglecting any possible coupling to other vibrational modes. [b] Reference 38. [c] Reference 13. Average experimental values for $[H_6Cu_6(PPh_3)_6]$: d(Cu–Cu) = 2.48 Å ("equatorial" belt); 2.74 Å ("trans" faces).

Table IV. Energy Changes (ΔE in kJ mol^{-1}) for Reactions Resulting in the Formation of Various Copper and Gold Clusters

reacn	ΔE
$4Cu \rightarrow Cu_4$	−678
$6Cu \rightarrow Cu_6$	−1324
$6Au \rightarrow Au_6$	−1290[a]
$6[Cu(PH_3)] \rightarrow [Cu_6(PH_3)_6]$	−1412
$6Cu + 6PH_3 \rightarrow [Cu_6(PH_3)_6]$	−2039
$Cu_6 + 6PH_3 \rightarrow [Cu_6(PH_3)_6]$	−713
$Cu_6 + 6H \rightarrow [H_6Cu_6]$	−1853
$6CuH \rightarrow [H_6Cu_6]$	−1357
$[H_6Cu_6] + 6PH_3 \rightarrow [H_6Cu_6(PH_3)_6]$	−867
$6CuH + 6PH_3 \rightarrow [H_6Cu_6(PH_3)_6]$	−2224
$Cu_4 + C \rightarrow CCu_4$	−1382
$[Cu_6]^{2+} + C \rightarrow [CCu_6]^{2+}$	−830
$[Au_6]^{2+} + C \rightarrow [Au_6]^{2+}$	−666[a]
$[CCu_6]^{2+} + 6PH_3 \rightarrow [CCu_6(PH_3)_6]^{2+}$	−1598
$[CAu_6]^{2+} + 6PH_3 \rightarrow [CAu_6(PH_3)_6]^{2+}$	−1783[a]
$[CCu_4] + 4PH_3 \rightarrow [CCu_4(PH_3)_4]$	−678
$[CCu_4(PH_3)_4] + 2[Cu(PH_3)]^+ \rightarrow [CCu_6(PH_3)_6]^{2+}$	−843

[a] Reference 17c.

atom changes and the Cu–Cu bond length increases from Cu_6 to $[H_6Cu_6]$ (see section 3.3). In the latter complex it is still significantly shorter than the values observed in $[H_6Cu_6(PPh_3)_6]$;[13] the calculated Cu–H distance equals almost exactly the average Cu–H distance found experimentally for $[H_6Cu_6(PPh_3)_6]$.[13] Note the increase in the Cu–H bond length from CuH to $[H_6Cu_6]$, as would be expected for a change in the hydrogen atom bonding mode from terminal to triply bridging. If a relaxation of the Cu_6 core from its octahedral symmetry had been allowed in the optimization, a further lowering of the energy may have resulted at the expense of a lengthening of the Cu–Cu bonds across the "trans" triangular faces.

The formation of $[H_6Cu_6(PH_3)_6]$ from CuH and PH_3 is rather exoenergetic, the greater part of the energy change for this reaction coming from the association of six CuH molecules to yield $[H_6Cu_6]$. The additional stabilization of the cluster by complexation with PH_3 results in an energy change which is comparable in magnitude to that calculated for the addition of the third or fourth molecules of PH_3 in $[Cu(PH_3)_4]^+$ (Tables II and IV). Comparing the formation energy of $[Cu_6(PH_3)_6]$ from 6 (Cu + PH_3) to that of $[H_6Cu_6(PH_3)_6]$ from 6 (CuH + PH_3), we note a stabilizing effect of the 6 hydride moieties, in agreement with the MO arguments expounded in the Introduction. The Cu–Cu bond length in $[H_6Cu_6(PH_3)_6]$ (Table III) is identical to the average of those observed for the "equatorial belt" in $[H_6Cu_6(PPh_3)_6]$ but significantly less than the average observed for the "trans faces" in this compound.[13] The observed distortions in several $[H_6Cu_6L_6]$ complexes with L = PPh_3 or substituted PPh_3, and in different solvates of the same complex, differ significantly[7-13] and so are possibly determined—at least in part—by crystal packing forces. The calculated Cu–Cu bond length in $[H_6Cu_6(PH_3)_6]$ is longer than that in $[Cu_6(PH_3)_6]$ or $[H_6Cu_6]$ (Table III). Again, their change is in contrast to the trend of the formation energies as discussed above. The calculated Cu–H bond length in $[H_6Cu_6(PH_3)_6]$ is the same as that in $[H_6Cu_6]$, and both are nearly identical to the average value observed in $[H_6Cu_6(PPh_3)_6]$.[13] The Cu–P distance (2.12 Å) is shorter than the average of the experimentally observed values for $[H_6Cu_6(PPh_3)_6]$ (2.226 Å)[13] but comparable to the value calculated for $[Cu(PH_3)]^+$ (2.14 Å; Table I).

The Cu–H bond stretching frequencies calculated for $[H_6Cu_6]$ and $[H_6Cu_6(PH_3)_6]$ (Table III) are considerably lower than that for diatomic CuH. The frequency ν(Cu–H) = 1363 cm^{-1} calculated for $[H_6Cu_6]$ is very close to the value 1400 cm^{-1} which has been assigned to the symmetric stretching vibration of a hydrogen atom chemisorbed on a triply bridging site on the Cu(111) surface.[41] The ν(Cu–H) vibrations in $[H_6Cu_6(PPh_3)_6]$ or related complexes with substituted PPh_3 ligands have never been assigned, presumably because of the low intensity and/or large width of the bands in the infrared spectra; it is often found that bands due to the ν(M–H) modes of bridging hydrides in transition metal hydride complexes are not observed in the infrared.[42] However, the complex $[H_4Co_4(\eta^5\text{-}C_5H_5)_4]$, which contains triply bridging hydrides on each of the four faces of a Co_4 tetrahedron, shows a ν(Co–H) band in the infrared at 950 cm^{-1},[43] which is close to the value of about 990 cm^{-1} obtained in the present work for $[H_6Cu_6(PH_3)_6]$.

We now turn to a discussion of the carbon-centered copper clusters. The Cu–Cu distance calculated for $[CCu_6(PH_3)_6]^{2+}$ is substantially longer than that obtained for the other clusters containing the Cu_6 unit (Table III). This is no doubt a consequence of the spatial requirements of the carbon atom; the resulting Cu–C distance (1.86 Å) is nevertheless quite short. For example, it is significantly shorter than that observed in the complexes bis(dimethylphosphonium bismethylide)dicopper, $[Me_2P(CH_2)_2Cu]_2$ (1.96 Å),[44] and tetrakis(trimethylphosphine)copper(I) dimethylcuprate(I), $[(Me_3P)_4Cu][Me_2Cu]$ (1.94 Å).[25] It is, however, comparable to the Cu–C bond lengths observed in some copper(I) complexes with carbonyl or isocyanide ligands (1.7–1.9 Å).[45] A Cu–C distance of 1.94 Å has been

(41) McCash, E. M.; Parker, S. F.; Pritchard, J.; Chesters, M. A. *Surf. Sci.* **1989**, *215*, 363.
(42) Copper, C. B.; Shriver, D. F.; Onaka, S. *Adv. Chem. Ser.* **1977**, *No. 167*, 232.
(43) Müller, J.; Dorner, H. *Angew. Chem.* **1973**, *85*, 867; *Angew. Chem., Int. Ed. Engl.* **1973**, *12*, 843.
(44) Schmidbaur, H.; Adlkofer, J.; Buchner, W. *Angew. Chem.* **1973**, *85*, 448; *Angew. Chem., Int. Ed. Engl.* **1973**, *12*, 415. Nardin, G.; Randaccio, L.; Zangrando, E. *J. Organomet. Chem.* **1974**, *74*, C23.
(45) Bauer, H.; Faust, J.; Froböse, R.; Füssel, J.; Krüerke, U.; Kunz, M.; Somer, H. M. *Gmelin Handbook of Inorganic Chemistry. Copper. Organocopper Compounds*; Part 4, Ed. Froböse, Füssel, J., Eds.; sprinter-Verlag: Berlin, 1987; Part 4, pp 110, 123.

calculated for the copper(I) species $[CuCH_3]$ and $[CuCO]^+$,[46,47] but these values may be somewhat overestimated as a consequence of the computational method (see above). The copper–phosphine bond energy in $[CCu_6(PH_3)_6]^{2+}$ is quite high (Table IV) and is comparable in magnitude to the average Cu–P bond energy in $[Cu(PH_3)_4]^+$ (Table II).

The species $[CCu_6(PH_3)_6]^{2+}$ is a model for the as yet unknown copper analogue of the gold complex $[CAu_6(PPh_3)_6]^{2+}$.[1,4] Attempts to prepare $[CCu_6(PPh_3)_6]^{2+}$ in a reaction analogous to that used for the preparation of the corresponding gold complex[1] have so far been unsuccessful. This reaction and others involving different tertiary phosphine ligands result in the deposition of metallic copper.[48a] Without a knowledge of the identity of the other decomposition products, no more can be said from the model calculations about the absolute stability of the carbon-centered Cu_6 cluster. But judging from the calculated formation energy of $[CCu_6(PH_3)_6]^{2+}$ which is almost as large as that found for $[CAu_6(PH_3)_6]^{2+}$ (Table III), one would not anticipate electronic factors to prevent the synthesis of the copper analogue of $[CAu_6(PPh_3)_6]^{2+}$.

The fact that $[CAu_6(PPh_3)_6]^{2+}$, in which the C atom displays the unusual coordination number 6, was formed in reactions which might have been expected to yield the as yet unknown compound $[CAu_4(PPh_3)_4]$, where the C atom displays its normal maximum coordination number 4, suggests that the binding of two $[Au(PPh_3)]^+$ units to $[CAu_4(PPh_3)_4]$ is strongly favoured energetically. (The related tricyclohexylphosphine complex could be obtained recently,[48b] where steric effects prevent the electrophilic attack by a fifth or sixth $(c\text{-}C_6H_{11})_3PAu^+$ reagent.) The term "aurophilicity" was coined to describe this phenomenon,[1] and part of the driving force for the expansion of the coordination number of the C atom from 4 to 6 was considered to be an attraction between the gold atoms surrounding the C atom.[1,4] It is of interest to study the analogous copper compounds. We have therefore carried out calculations on the species $[CCu_4(PH_3)_4]$ in order to investigate its stability relative to $[CCu_6(PH_3)_6]^{2+}$, and the results of these calculations are given in Tables III and IV. The energy change for the reaction

$$[CCu_4(PH_3)_4] + 2[Cu(PH_3)]^+ \rightarrow [CCu_6(PH_3)_6]^{2+} \qquad (3)$$

is substantial, -843 kJ mol^{-1}. LCGTO–LDF calculations on the octahedral hypercoordinated carbon species $[CLi_6]^{2+}$ show that the analogous reaction

$$CLi_4 + 2Li^+ \rightarrow [CLi_6]^{2+} \qquad (4)$$

is exoenergetic by -296 kJ mol^{-1},[28] in good agreement with results from a previous ab initio study (-300 kJ mol^{-1}).[49] This value is considerably smaller in magnitude than the value calculated here for reaction 3.

There is a decrease in the Cu–Cu distance from 3.01 Å in $[CCu_4(PH_3)_4]$ to 2.63 Å in $[CCu_6(PH_3)_6]^{2+}$. The corresponding Cu–C distances for these two species are 1.85 and 1.86 Å respectively. Thus, the Cu–C distance hardly changes at all with an increase in the coordination number of the C atom from 4 to 6. The Cu–Cu distance of 2.63 Å in $[CCu_6(PH_3)_6]^{2+}$ is significantly larger than the value 2.35 Å observed in [(tolyl-NNNNN-tolyl)Cu]$_3$, the shortest Cu–Cu distance yet observed in a copper(I) complex.[50] The existence of a significant Cu–Cu bonding interaction at such a short distance has been proposed,[51] but the contrary proposal has also been made,[52,53] and the existence of bonding interactions at longer distances such as those observed in the present study is still more questionable.

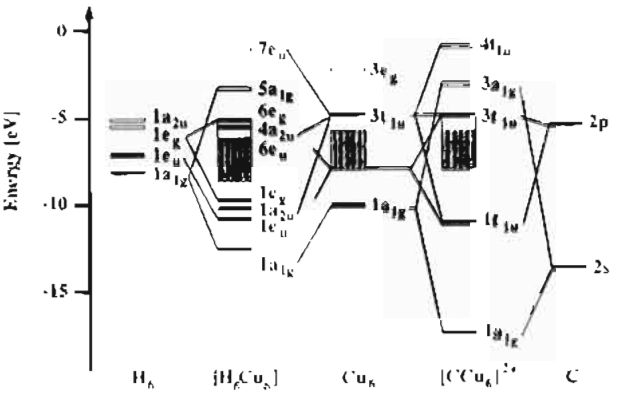

Figure 5. Energy level and interaction diagram for the valence molecular orbitals of Cu_6, $[H_6Cu_6]$, and $[CCu_6]^{2+}$ as well as H_6 and C. The spectrum of $[CCu_6]^{2+}$ has been shifted upward uniformly by 10 eV. Occupied levels are displayed as a solid line; empty ones are shown as an open narrow box. The manifold of the Cu 3d orbitals is shown as a box wherein levels important for the metal–ligand interaction are given explicitly; the rest is indicated by shading.

3.3. Comparison of the Bonding in $[H_6Cu_6]$ and $[CCu_6]^{2+}$ Complexes. It was mentioned in the Introduction that a formal relationship exists between the electronic structures of $[H_6M_6L_6]$ and $[CM_6L_6]^{2+}$. These complexes can both be regarded as derivatives of the $[M_6L_6]$ unit, in which the six M–M bonding electrons are stabilized by bonding to six H atoms in the former case and to a C^{2+} unit in the latter case. The same is true of the fragments $[H_6M_6]$ and $[CM_6]^{2+}$ in relation to the parent M_6 cluster, and the electronic structures of these species with M = Cu are compared in Figure 5 by means of the LCGTO–LDF valence MO energy level diagrams. For Cu_6, the lowest energy valence orbital ($1a_{1g}$) and the HOMO ($3t_{1u}$) are mainly Cu 4s in character. Between these two levels lies a manifold containing the levels of predominantly Cu 3d character. The remaining orbitals of Cu 4s character form the LUMO ($3e_g$).

In $[H_6Cu_6]$, the symmetry of the cluster is lowered from O_h to D_{3d}, and the t_{1u} HOMO of Cu_6 formally splits into the orbitals of type $a_{2u} + e_u$. The six H 1s orbitals induce MOs of symmetry $a_{1g} + e_g + a_{2u} + e_u$, matching in symmetry the MOs resulting from the six Cu 4s orbitals. As a consequence, six hydride bonding levels $1a_{1g}$, $1e_u$, $1a_{2u}$, and $1e_g$ are formed involving Cu 4s and some Cu 3d contributions (Figure 5). The formation of the Cu–H bonding MO $1e_g$ is somewhat surprising since its metal contribution is of pure Cu 3d character. The cluster orbital $1a_{1g}$ preserves most of its character in Cu_6 and is responsible for much of the Cu–Cu bonding.

In $[CCu_6]^{2+}$ full octahedral symmetry is retained. The symmetries of the C 2s and 2p orbitals are a_{1g} and t_{1u}, respectively, and these match the symmetries of orbitals of the Cu_6 cluster which are derived from the Cu 4s orbitals. Bonding molecular orbitals $1a_{1g}$ and $1t_{1u}$ are thus formed, the former being largely of C 2s character (Figure 5; the spectrum has been shifted upward by 10 eV to compensate for the effect of the charge on this cluster and to facilitate a comparison with the other uncharged clusters). The 4s-type MOs of Cu_6, $1a_{1g}$ and $3t_{1u}$, are pushed upward by this interaction and become formally empty. The $3t_{1u}$ MO of $[CCu_6]^{2+}$ belongs formally to the Cu 3d manifold, and it weakens the Cu–C bond through its Cu 4s contribution. In $[H_6Cu_6]$, on the other hand, we have four hydride levels, one of which ($1e_g$)

(46) Bauschlicher, C. W.; Langhoff, S. R.; Partridge, H.; Barnes, L. A. *J. Chem. Phys.* **1989**, *91*, 2399.
(47) Barnes, L. A.; Rosi, M.; Bauschlicher, C. W. *J. Chem. Phys.* **1990**, *93*, 609.
(48) (a) Steigelmann, O.; Schmidbaur, H.; Bowmaker, G. A. Unpublished results. (b) Steigelmann, O.; Schmidbaur, H. Unpublished results.
(49) Jemmis, E. d.; Chandrasekhar, J.; Würthwein, E.-U.; Schleyer, P.v.R. *J. Am. Chem. Soc.* **1982**, *104*, 4275.
(50) Beck, J.; Strähle, J. *Angew. Chem.* **1985**, *97*, 419; *Angew. Chem., Int. Ed. Engl.* **1985**, *24*, 409.
(51) Merz, K. M.; Hoffmann, R. *Inorg. Chem.* **1988**, *27*, 2120.
(52) Cotton, F. A.; Xuejun Feng, Matusz, M.; Poli, R. *J. Am. Chem. Soc.* **1988**, *110*, 7077.
(53) Kölmel, C.; Ahlrichs, R. *J. Phys. Chem.* **1990**, *94*, 5536.

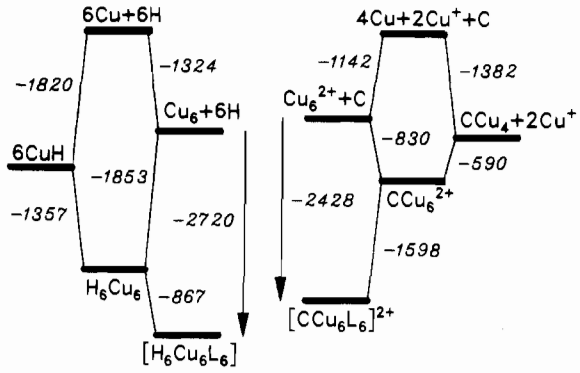

Figure 6. Comparison of calculated energy changes (in kJ mol^{-1}) for the reactions 6H + 6Cu + 6PH_3 → $[H_6Cu_6(PH_3)_6]$ (left scheme) and C + 4Cu + 2Cu^+ + 6PH_3 → $[CCu_6(PH_3)_6]^{2+}$ (right scheme). For reasons of clarity, the six ligands L = PH_3 are mentioned explicitly only in the products.

has no formal symmetry equivalent in $[CCu_6]^{2+}$. Thus, there are some significant differences compared to the electronic structure of the cluster $[H_6Cu_6]$ (see below).

The energy range of the 3d manifold in $[CCu_6]^{2+}$ is approximately equal to that for Cu_6. This is perhaps surprising, as the equilibrium Cu–Cu distance in $[CCu_6]^{2+}$ is somewhat larger than that for Cu_6 (Table III), resulting in a reduced interaction between the 3d orbitals in the former case. Although there are Cu 3d cluster orbitals of a_{1g} and t_{1u} symmetry, these do not overlap very strongly with the C 2s or 2p orbitals, so that the orbitals within the 3d manifold have essentially no C 2s or 2p character. The main difference between the 3d orbitals for Cu_6 and those for $[CCu_6]^{2+}$ is the greater degree of d–s mixing in the latter case. In the orbital $2a_{1g}$, for example, the ratio of the Cu 4s to Cu 3d populations increases from 0.29 in Cu_6 to 0.55 in $[CCu_6]^{2+}$. It has been shown previously that the degree of d–s mixing increases in the presence of strongly coordinated axial ligands,[4,51,54] and it is clear from the above results that the C atom has just this effect on the copper orbitals in $[CCu_6]^{2+}$. Admixture of higher energy s and p orbitals into the d shell results in a stabilization of both the bonding and antibonding d orbital combinations and leads to the possibility of an attractive metal–metal interaction. However, this is largely excluded due to the metal–metal distance in this cluster (Table III). The bonding in $[CCu_6]^{2+}$ is essentially the same as that previously described for $[CAu_6]^{2+}$.[1,4]

The various energy changes reflect this difference in Cu–ligand bonding in the two clusters rather dramatically (see Figure 6). The reaction

$$Cu_6 + 6H \rightarrow [H_6Cu_6] \qquad (5)$$

is highly exoenergetic, −1853 kJ mol^{-1}, whereas only 830 kJ mol^{-1} is released in

$$[Cu_6]^{2+} + C \rightarrow [CCu_6]^{2+} \qquad (6)$$

However, no low-lying Cu–Cu bonding cluster orbitals are perturbed during the formation of $[CCu_6(PH_3)_6]^{2+}$,

$$[CCu_6]^{2+} + 6PH_3 \rightarrow [CCu_6(PH_3)_6]^{2+} \qquad (7)$$

whereas in the reaction

$$[H_6Cu_6] + 6PH_3 \rightarrow [H_6Cu_6(PH_3)_6] \qquad (8)$$

the Cu–PH_3 bonding is partially offset by the loss of Cu–Cu bonding character of the low-lying valence orbitals of $[H_6Cu_6]$, thus the remarkably low value of the corresponding energy change, −867 kJ mol^{-1}. The corresponding changes in the Cu–Cu bond lengths (Table III) corroborate this analysis. It is worth noting

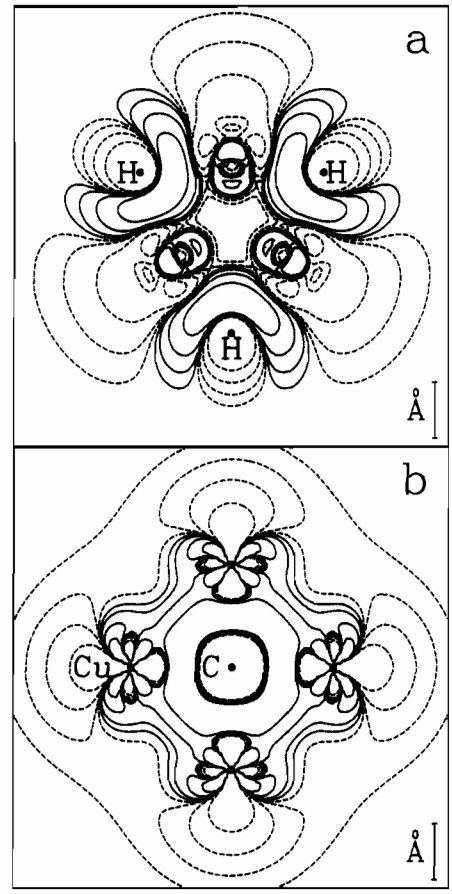

Figure 7. Electron density difference maps $\Delta\rho = \rho(AB) - \rho(A) - \rho(B)$ for (a) $[H_6Cu_6]$ (A = Cu_6, B = H_6) and (b) $[CCu_6]^{2+}$ (A = Cu_6^{2+}, B = C). The reference density $\rho(A) + \rho(B)$ is formed from orthogonalized fragment orbitals. For $[H_6Cu_6]$, a plane perpendicular to the 3-fold axis is shown which contains three hydrogen atoms; for $[CCu_6]^{2+}$, the plane contains the central carbon atom and four copper atoms. The positions of the atoms are marked by dots. The contour values are ±0.00032, ±0.001, ±0.0032, and ±0.01; negative values are indicated by a dashed line.

that the total formation energies of $[H_6Cu_6(PH_3)_6]$ [5,8] and $[CCu_6(PH_3)_6]^{2+}$ [6,7] are quite comparable (see Figure 6).

Further insight into the bonding of the clusters $[H_6Cu_6]$ and $[CCu_6]^{2+}$ is provided by electron density difference maps (Figure 7) which illustrate the charge rearrangement due to the formation of the Cu–H and Cu–C bonds, respectively. The reference density is formed from a wave function of the superimposed fragments (Cu_6 and H_6 as well as Cu_6^{2+} and C) where the orbitals have been properly orthogonalized. The contour plot for $[H_6Cu_6]$ (Figure 7a) is shown for a plane which contains three hydrogen atoms and is perpendicular to the main 3-fold axis. The charge density of diffuse Cu 4s character is reduced overall but accumulated in the Cu–H bonding area. The hydrogen atoms appear strongly polarized but do attract charge from the metal in agreement with the formation of a hydride. Given the rather extended nature of the Gaussian basis set, Mulliken populations do not provide an unambiguous characterization of the charge distribution within the cluster. However, the charge transfer from Cu to H can be inferred from the change of the dipole moment when one H atom is moved perpendicular to the plane of its three metal neighbors. The corresponding "dynamic dipole moment", which may be interpreted as an effective charge[55] ($q_{eff}(H) = -0.13$ e), confirms the hydride character of the complex.

For the system $[CCu_6]^{2+}$ (Figure 7b), one of the planes containing the central carbon atom and four of its Cu neighbors

(54) Bowmaker, G. A.; Boyd, P. D. W.; Sorrenson, R. J. *J. Chem. Soc., Faraday Trans. 2* **1985**, *81*, 1627.

(55) Rösch, N. In *Cluster Models for Surface and Bulk Phenomena*; Pacchioni, G., Bagus, P. S., Parmigiani, F., Eds.; NATO ASI Series B, Vol. 283; Plenum: New York, 1992; p 251.

is shown. In this case, the reference fragment Cu_6^{2+} was derived from the Cu_6 cluster by reducing the occupation of the HOMO appropriately. From Figure 7b it is obvious that the interaction of the copper cluster with the central carbon atom leads to a charge transfer into the bonding area at the expense of diffuse Cu 4s-type charge density, quite similar to the case of $[H_6Cu_6]$.

While the above results suggest no absolute reason for the apparent nonexistence of $[CCu_6]^{2+}$ complexes, the somewhat greater relative stability of $[H_6Cu_6]$ complexes can be understood in terms of the bonding description given above. Thus, the lower symmetry and different topology of the $[H_6Cu_6]$ unit allows participation of the Cu 3d orbitals in the Cu–H bonding as well as in the Cu–Cu bonding. This contrasts with the case of the $[CCu_6]^{2+}$ unit, in which the topology is such that essentially no favorable overlap between the C 2s and 2p orbitals with the Cu 3d orbitals occurs. The energy changes, even if overestimated in the present LDF approach, do provide a relative measure for the stability of the various cluster compounds. The total formation energies of the cluster compounds $[H_6Cu_6(PH_3)_6]$, $[CCu_6(PH_3)_6]^{2+}$, and $[CAu_6(PH_3)_6]^{2+}$ from their atomic (ionic) constituents are 4044, 3570, and 3715 kJ mol^{-1} (Table IV and ref 17c). Thus, the present results suggest that $[CCu_6]^{2+}$ is the least stable of the species $[H_6Cu_6]$, $[CCu_6]^{2+}$, and $[CAu_6]^{2+}$ and may explain why attempts to prepare complexes of this type have so far been unsuccessful.

Acknowledgment. We thank A. Görling, T. Fox, and O. Häberlen for many discussions and for their assistence during various phases of this work. G.A.B. acknowledges the grant of a period of study leave from the University of Auckland and the grant of a research fellowship by the Alexander von Humboldt Foundation, Germany. N.R. acknowledges the grant of a visiting professorship at the University of Auckland, during the tenure of which this work was completed. This work was supported by the Deutsche Forschungsgemeinschaft, the Fonds der Chemischen Industrie, and the Bund der Freunde der TU München.